Research on CRM Boost PFC Converter Based on GaN Device

Yao Ding[1,2] and En Fang[1,2(✉)]

[1] School of Electrical and Control Engineering, Xuzhou University of Technology, Xuzhou 221018, Jiangsu, China
fangen@cumt.edu.cn

[2] Jiangsu Key Construction Laboratory of Large Engineering Equipment Testing and Control Technology, Xuzhou 221018, Jiangsu, China

Abstract. There is a need for Power Factor Correction (PFC) converters to improve performance and reduce device size while maintaining a high power factor in the consumer electronics arena. Increasing the switching frequency is the essential way to increase the power density of the PFC converter. When the switching frequency of the converter is close to the MHz level, the switching loss of the conventional Si MOSFET increases sharply, resulting in a decrease in the overall efficiency of the converter. The dual-pulse test platform based on the cascode GaN transistor TPH3206PD and the experimental platform of 200 W single-phase CRM boost PFC converter is introduced. Then, the stability of the high-frequency driving circuit of the GaN device is verified by the dual-pulse test platform, which effectively avoids the false turn-off phenomenon in the turn-on process. The switching loss of TPH3206PD is measured experimentally, and the accuracy of theoretical calculation is verified. The experimental results show that when the operating frequency of the CRM boost PFC converter is close to 1 MHz. GaN devices can effectively reduce switching loss and improve overall efficiency.

Keywords: Boost PFC converter · Critical current mode · GaN devices

1 Introduction

The performance of switch-mode power supply (SMPS) is the key to the reliable operation of power equipment. Among the performance parameters of SWPs, the power factor (PF) is the most crucial parameter for energy saving and environmental protection. PF is the ratio of active power to total power. The reduction of PF means an increase in power consumption and harmonic pollution, which leads to circuit failure, equipment damage, and electromagnetic interference. Power Factor Correction (PFC) improves the harmonic generation equipment in rectification, which is the primary method to solve the problem of low PF. PFC converter improves pf value, makes input current and input voltage in phase, corrects the input current waveform, and reduces distortion and harmonics. It is more and more necessary for power conversion equipment to improve

D. Jiang and H. Song (Eds.): SIMUtools 2021, LNICST 424, pp. 165–177, 2022.
https://doi.org/10.1007/978-3-030-97124-3_15

efficiency and minimize module size while maintaining or improving electrical and thermal performance in consumer electronics. At the same time, following the development concept of socialism with Chinese characteristics in the new era, power products have the development goals of high efficiency and miniaturization. The volume of the PFC converter usually accounts for a large percentage of power supply equipment, which directly affects the power density of the power adapter. In response to the advocacy of gradually building energy consumption mode of saving, efficient, clean, and low-carbon society, improving the efficiency and power density of PFC converter is an effective way to realize efficient and clean power products.

2 Analysis of Theory of CRM Boost PFC Converter Based on GaN Device

The cascode GaN transistors are more suitable for Critical Current Mode (CRM) boost PFC Converters. Analyzing and comparing the static characteristics of the cascode GaN transistors and Si devices can help to analyze the conducting losses of both. The principle analysis of GaN devices and CRM boost PFC converters is the basis of applying GaN devices to high-frequency CRM boost PFC converters. Therefore, the static characteristics of the cascode GaN transistors and Si devices are analyzed and compared in this paper. The power factor correction principles with switching mode and steady-state for the CRM boost PFC converters are discussed.

2.1 Static Characteristics of Cascode GaN Transistors

The cascode GaN transistor TPH3206PD (600 V/17 A/150 mΩ) of Transphorm company is selected as the research object. TPH3206PD is composed of Si MOSFET IRF8707 and depletion GaN HEMT via the cascode packaging technology. Their parameters are shown in Table 1. The drain-source voltage $V_{\text{ds-Si}}$ of Si MOSFET is used as the driving voltage of GaN HEMT. In order to cut off the drain current of GaN HEMT, it is necessary to select Si MOSFET with enough breakdown voltage to meet condition $V_{\text{dsmax\_Si}} > |V_{\text{th\_GaN}}|$ for turning off the GaN HEMT. GaN HEMT has an insulator between the gate electrode and the AlGaN barrier layer, selecting Si MOSFET with high breakdown voltage. It shows that the cascode structure can drive the GaN HEMT with a large dv/dt. As shown in Table 1, the rated voltage V_{dss} of IRF8707 is 30 V, and the absolute value of threshold voltage of GaN HEMT $|V_{\text{th\_GaN}}|$ is 20 V, which meets the academic requirements.

Table 1. Parameters table of Cascode GaN transistor and its components.

Parameters	TPH3206PD	Depletion GaN HEMT	IRF8707
Rated voltage V_{dss}	600 V	600 V	30 V
Rated current I_d(T_c = 25 °C)	17 A	17 A	17 A
Conducting resistance R_{ds_on}	150 mΩ	140 mΩ	11.9 mΩ
Threshold voltage V_{th}	2.1 V	−20 V	2.1 V
Gate source voltage V_{gs}	−18 V–18 V	−40 V–2 V	−20 V–20 V

Output Characteristics of Si MOSFET IRF8707

Si MOSFET IRF8707 is a bidirectional conducting device with a parasitic diode, so its output characteristic curve includes the first and third quadrant. Figure 1 shows the output characteristic curves of Si MOSFET IRF8707. The first quadrant curve shows the relationship between voltage and current when the device is in forwarding conduction. The third quadrant curve shows the relationship between voltage and current when the device is under reverse voltage.

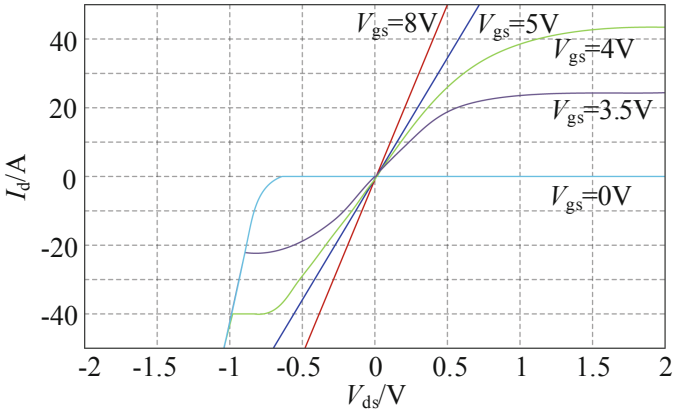

Fig. 1. Output characteristic curve of Si MOSFET IRF8707.

When the Si MOSFET is under forwarding voltage, the driving voltage V_{gs_Si}, larger than the threshold voltage, is applied to the gate-source and the device is on. Under the same voltage, the higher the driving voltage is, the smaller the on-resistance and the smaller the conducting state loss is. When the driving voltage applied to the gate-source is 8 V, the output characteristic is approximately linear.

When Si MOSFET withstands reverse voltage, if V_{gs_Si} is less than V_{th_Si}, the conduction channel of Si MOSFET is blocked, and the current flows through the body diode of the device. The device shows diode characteristics, and the reverse voltage drop of the device is the body diode voltage drop V_F. Suppose the gate-source driving voltage is large enough, the reverse conduction resistance of the device decreases. When the

reverse current flows through the channel, the voltage drop of the source and drain is V_{sd_Si}. The output characteristic curve of Si MOSFET is almost symmetrical with the first quadrant. V_{gs_Si} is greater than its threshold voltage V_{th_Si}. At this time, current flows through both the channel and the bulk diode, and the device works in the reverse saturation region. The reverse conduction voltage is clamped as the voltage drop of the bulk diode V_F.

Output Characteristics of Depletion GaN HEMT

There is no parasitic diode in the lateral structure of depletion GaN HEMT, which determines the symmetry of its conduction characteristics, i.e., gate-source voltage V_{gs_GaN} and gate-drain voltage V_{gd_GaN} can drive the device on and off.

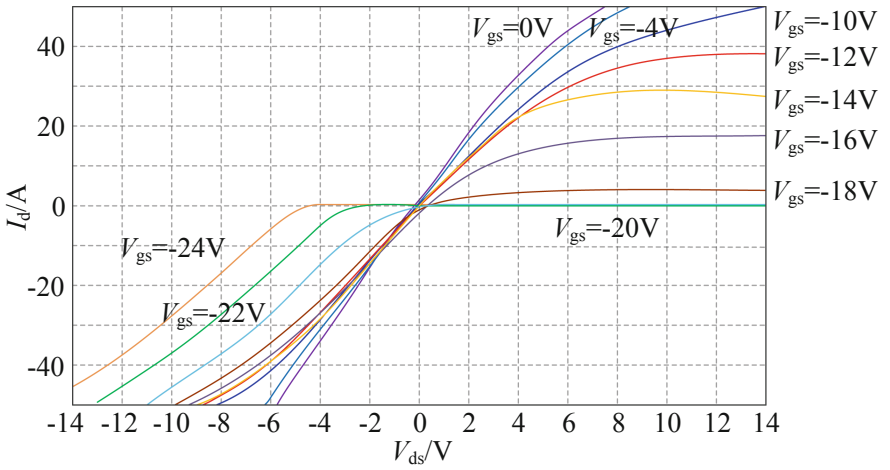

Fig. 2. Output characteristic curve of depletion GaN HEMT.

Figure 2 shows the first and third quadrant output characteristic curves of depletion GaN HEMT in TPH3206PD. It can be seen that the output characteristic curve of depletion GaN HEMT in the third quadrant is different from that of Si MOSFET due to the absence of parasitic diode and its symmetrical conduction characteristics. Because there is no bulk diode in GaN HEMT, the reverse conduction characteristics are obviously different from that of Si MOSFET, which leads to the difference between the cascode GaN transistor and Si MOSFET.

Figure 3 shows the output characteristic curve of TPH3206PD. It can be seen that the output characteristics of the cascode GaN transistor are similar to that of power Si MOSFET in the first quadrant. Still, it does not show diode characteristics in the case of reverse conduction in the third quadrant. It is mainly because the cascode GaN transistor has a cascode structure. Its reverse conduction voltage is the sum of reverse conduction voltage of power Si MOSFET and depletion GaN HEMT. Therefore, the reverse conduction voltage of the cascode Gan transistor is slightly higher than that of Si MOSFET of the same voltage level.

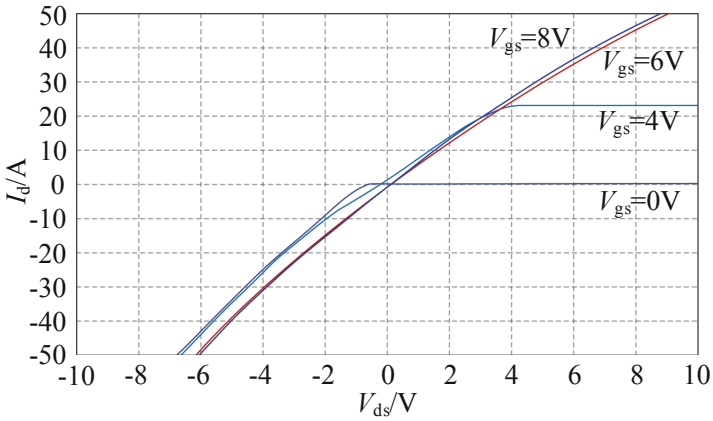

Fig. 3. Output characteristic curve of TPH3206PD.

2.2 Comparison of Static Characteristics Between the Cascode GaN Transistor and Si Device

According to the difference of static characteristics between the cascode GaN transistor and Si devices, the super junction Si MOSFET of Infineon CoolMOS IPP65R125C7 (650 V/13 A/125 mΩ) as representatives of current high-performance Si devices are selected. The rated voltage and current are similar to TPH3206PD, which is suitable for comparative analysis. Some parameters of TPH3206PD and IPP65R125C7 are shown in Table 2.

The conduction characteristics of the cascode GaN transistor TPH3206PD at different working junction temperatures of $T_J = 25$ °C and 175 °C are shown in Figs. 2, 3 and 4. It can be seen that in the actual operating range of 0–17 A, the conduction characteristics can be approximately linear. The R_{ds_on} value at any temperature can be calculated from Fig. 4 by the ratio of V_{ds} to I_d in the linear region.

The R_{ds_on} performance of Si device IPP65R125C7 is 0.057–0.150 Ω, 38%–100% better than that of the cascode GaN transistor in the same condition.

3 Analysis of Basic Principles of CRM Boost PFC Converter

The basic principle of a single-phase CRM boost PFC converter consists of two parts. The first part is the working mode of main switch S in a switching cycle, and the second part is the principle of power factor correction. The central circuit topology of the single-phase boost PFC converter is shown in Fig. 5. The primary circuit includes AC power supply v_{in}, EMI filter, rectifier bridge, boost filter inductor L, switch S, diode D, input capacitor C_{in}, output regulator capacitor C_o and load, etc.

3.1 Analysis of CRM Boost PFC Converter

Figure 6 shows the equivalent circuit of the converter when the switch is on and off. Figure 7 shows the changes in switch voltage, inductance current, and voltage. At $t = t_0$,

Table 2. Partial parameters of TPH3206PD and IPP65R125C7.

Parameters	Transphorm TPH3206PD	Infineon IPP65R125C7
Technology type	Cascade GaN transistor	Superjunction Si MOSFET
Rated voltage V_{ds}	600 V	650 V
Rated current I_d ($T_c = 25$ °C)	17 A	13 A
Conducting resistance R_{ds_on}	150 mΩ	125 mΩ
Gate-source voltage V_{gs}	−18 V–18 V	−20 V–20 V
Threshold voltage V_{TH}	2.1 V	3.5 V
Input capacitance C_{iss}	760 pF	1670 pF
Output capacitance C_{oss}	44 pF	26 pF
Reverse transmission capacitor C_{rss}	34 pF	579 pF
Total charge of gate-source Q_{gs}	2.1 nC	8 nC
Total gate-drain charge Q_{gd}	2.2 nC	11 nC
Total gate-charge Q_g	6.2 nC	35 nC
Total reverse recovery charge Q_{rr}	54 nC	7 μC
Reverse recovery time t_{rr}	17 ns	800 ns

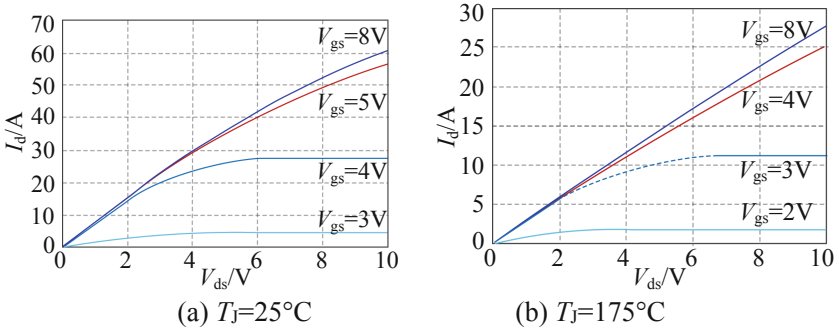

Fig. 4. Conduction characteristic of TPH3206PD at 25 °C and 175 °C.

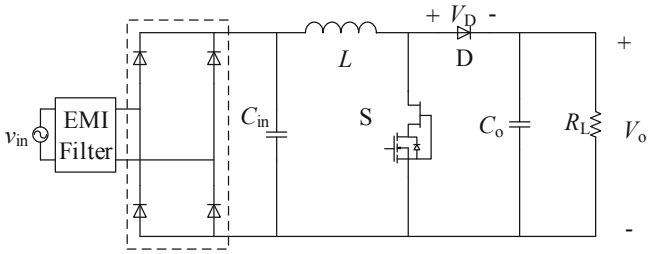

Fig. 5. Main circuit of single-phase Boost PFC.

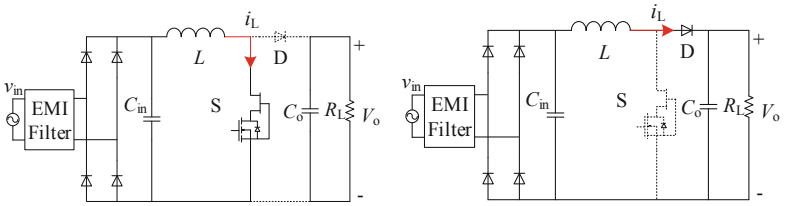

Fig. 6. Equivalent circuit of CRM Boost PFC working mode.

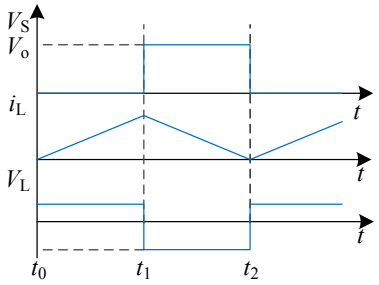

Fig. 7. Equivalent waveforms of CRM Boost PFC key parameters.

the switch S turns on, and the diode D turns off. The AC power v_{in} charges the inductor L, and C_o discharges the load R_L. The inductance current i_L rises from zero and can be calculated by Eqs. (1) and (2) between $[t_0, t_1]$.

$$L\frac{di_L}{dt} = |v_{in}| \tag{1}$$

$$v_{in} = V_{in}\sin\omega t = \sqrt{2}V_{RMS}\sin\omega t \tag{2}$$

Where, V_{in} is the peak value of AC power supply voltage, and V_{RMS} is the effective value of AC power supply voltage. ω is the angular frequency of the AC supply voltage.

In this stage, v_{in} can be considered as the instantaneous value of the AC power supply. Because the power frequency of the AC power supply is far less than the switching frequency, v_{in} is almost unchanged in a switching cycle. When $t = t_1$, the inductance current i_L rises to the peak i_{LP}. The growth of i_L is expressed as follows.

$$i_{LP} = \frac{|v_{in}|}{L}t_{on} \tag{3}$$

$$t_{on} = t_1 - t_0 \tag{4}$$

At $t = t_1$, switch S turns off, and diode D turns on. v_{in} and L charge C_o through D and discharge R_L at the same time. Inductance current i_L drops to 0 due to the discharge,

and the voltage drop of the switch is V_o. At this stage, the mathematical expression of inductance current i_L is Eq. (5).

$$L\frac{di_L}{dt} = |v_{in}| - V_o \tag{5}$$

At $t = t_2$, the inductance current i_L decreases to 0, and the inductance current i_L can be calculated when the next switching cycle begins.

$$i_{LP} = \frac{V_o - |v_{in}|}{L} t_{off} \tag{6}$$

$$t_{off} = t_2 - t_1 \tag{7}$$

3.2 Analysis of Steady-State of CRM Boost PFC Converter

The switching frequency is constantly changing. When analyzing the specific range of switching frequency, it is necessary to determine the input voltage, output voltage, boost inductance and output power of CRM boost PFC converter.

When the practical value of input voltage V_{RMS} is 220 V and the output voltage V_{out} is 390 V, if the input voltage reaches the peak value, the minimum switching frequency f_{s_min} is 1. Mathcad can be used to show the change curve of the switching frequency of AC power supply in one cycle, as shown in Fig. 8. It can be seen that the maximum frequency is about 4.5 times the minimum frequency. If the minimum switching frequency of the designed PFC converter is 200 kHz, the switching frequency range is about 200 kHz–900 kHz.

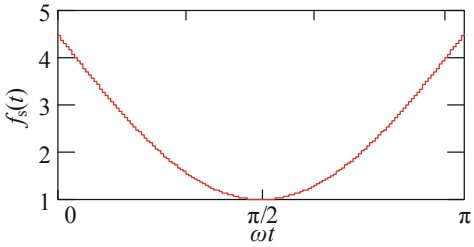

Fig. 8. Diagram of switching frequency variation.

4 Experimental Research

4.1 Dual-Pulse Test Platform

In order to verify the theoretical analysis results, a dual-pulse test apparatus based on the cascode GaN transistor TPH3206PD is built. And a 200 W single-phase CRM boost

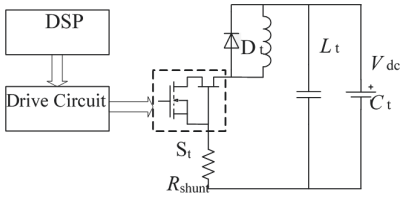

Fig. 9. Structure diagram of the dual-pulse test platform.

PFC converter experimental platform is made to verify the dynamic performance and loss of TPH3206PD. The control performance is proved, and power loss of CRM boost PFC converter based on GaN is calculated to prove the efficiency improvement. The input current zero-crossing distortion is suppressed.

Figure 9 is the structure diagram of the dual-pulse test platform, which includes driving circuit and DC power supply V_{dc}, filter capacitor C_t, inductance L_t, freewheeling diode D_t and switch S_t to be tested. Other parameters of the dual pulse test platform are shown in Table 3.

Table 3. Parameters table of double pulse test platform.

Parameter	Values
Input Voltage V_{dc}	390 V
Driving voltage V_{GS}	12 V
Driving resistor R_G	5 Ω, 20 Ω
Switching frequency f_{sw}	550 kHz

4.2 Cascode Gan Transistor Switching Loss Verification

In the dual-pulse test of the cascode GaN transistor, the current before turning on is zero, and the conducting current is 3.84 A, 2.04 A, 1.48 A, and 1.23 A, respectively. Four groups of switching waveforms are obtained by changing the switching current by changing the time of the first pulse, as shown in Figs. 10, 11, 12 and 13.

According to the switching waveforms, the switching losses of four groups of different switching currents are calculated and compared with the theoretical calculation. The theoretical and actual switching losses of TPH3206PD shown in Table 4 are obtained. The theoretical value of turn-on loss is quite different from the actual value because the turn-on process of TPH3206PD has a specific oscillation. In the experiment, the parasitic parameters caused by PCB layout are challenging to be quantified. So the oscillation waveform in the investigation is slightly different from that in the simulation, which causes the accuracy of the theoretical value of turn-on loss to be lower than that of turn-off loss. According to the parameters in Table 4, the maximum difference between the theoretical and actual values is 4.99%, and the minimum difference is 1.73%. The

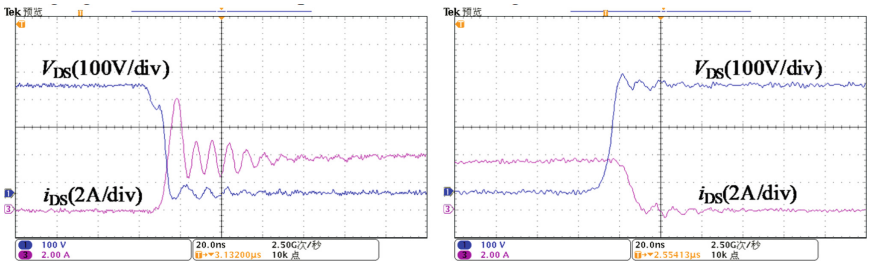

(a) Turn on (b) Turn off

Fig. 10. Switching waveforms when the switching current is 3.84 A.

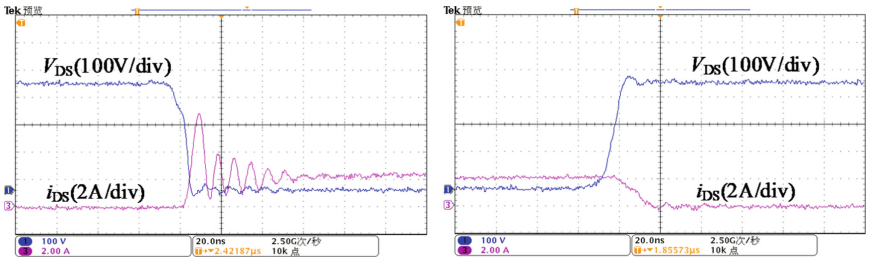

(a) Turn on (b) Turn off

Fig. 11. Switching waveforms when the switching current is 2.04 A.

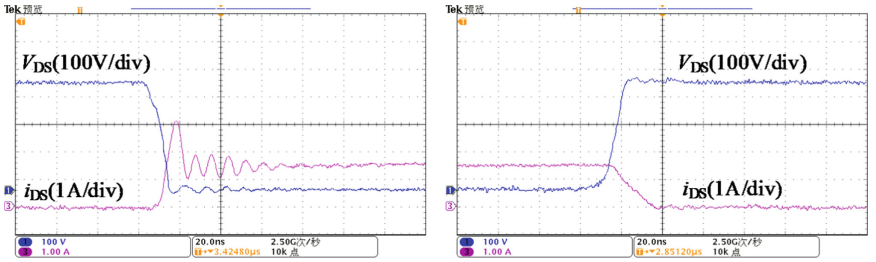

(a) Turn on (b) Turn off

Fig. 12. Switching waveforms when the switching current is 1.48 A.

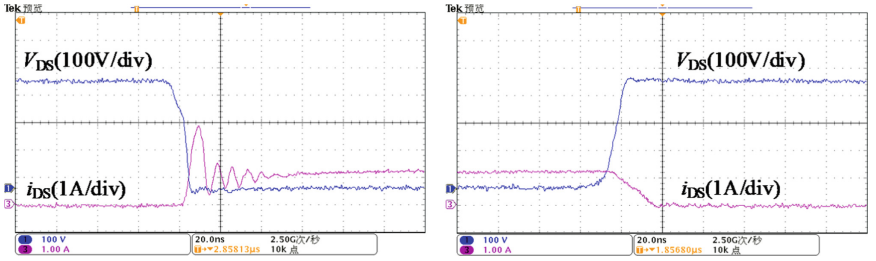

(a) Turn on (b) Turn off

Fig. 13. Switching waveforms when the switching current is 1.23 A.

leading difference between the theoretical and actual values is 3.71%, and the minimum difference is 0.08%. The accuracy of switching loss is within the allowable error range, which shows that the theoretical and simulation analyses are in line with reality.

Table 4. Comparison of theoretical and actual values of TPH3206PD switching.

	Theoretical turn-on loss/μJ	Actual turn-on loss/μJ	Theoretical turn-off loss/μJ	Actual turn-off loss/μJ
$i_{rms} = 3.84$ A	26.232	25.677	4.410	4.543
$i_{rms} = 2.04$ A	14.340	14.657	3.658	3.799
$i_{rms} = 1.48$ A	11.158	11.745	3.206	3.231
$i_{rms} = 1.23$ A	8.625	8.924	3.003	3.079

4.3 Experimental Analysis of Converter Performance

The converter reaches steady-state quickly. In order to test whether the CRM boost PFC converter based on GaN device can achieve the goals of high power factor and more than 90% efficiency in the entire input range, the VRMs of 85 V, 160 V, 220 V, and 265 V are selected for the experiment, and the results are shown in Fig. 14.

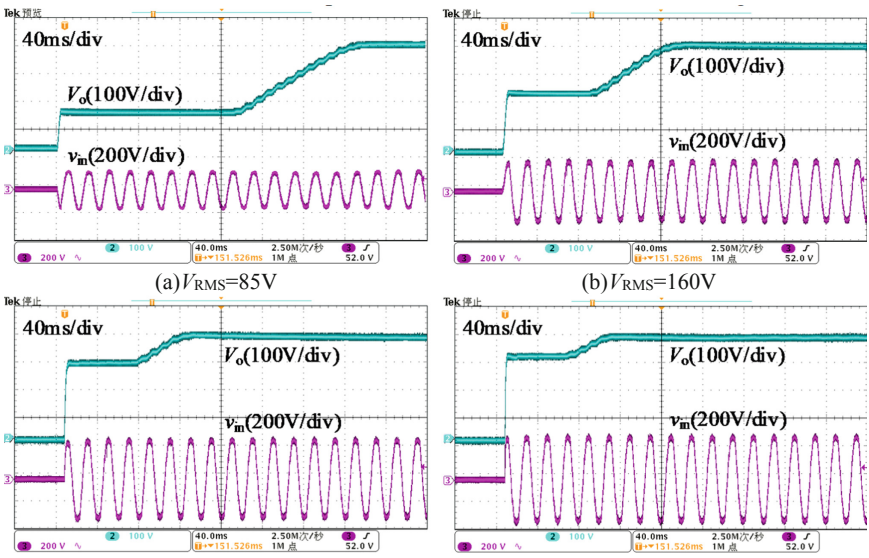

Fig. 14. Output waveforms of CRM Boost PFC converter under different input voltages.

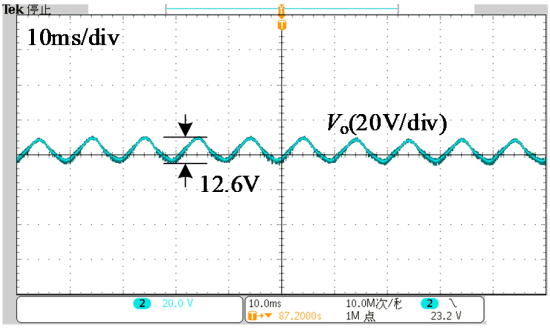

Fig. 15. Steady-state waveforms of output voltage.

When the CRM boost PFC converter reaches the steady-state, the output voltage waveform is shown in Fig. 15. The measured output voltage ripple is 12.6 V, less than 5%, which conform to the theoretical and simulation analyses.

5 Conclusions

The dual-pulse test platform based on the cascode GaN transistor TPH3206PD is built, and the experimental platform of a 200 W single-phase CRM boost PFC converter is described. Then, the stability of the high-frequency driving circuit of the GaN device is verified by the dual-pulse test platform, which effectively avoids the false turn-off phenomenon in the turn-on process. The switching loss of TPH3206PD is measured experimentally, and the accuracy of theoretical calculation is verified. The experimental results show that when the operating frequency of the CRM boost PFC converter is close to 1 MHz, GaN devices can effectively reduce the switching loss and improve the overall efficiency.

Acknowledgements. The authors acknowledge the Jiangsu University Natural Science Research Project (18KJB470024) and Provincial Construction System Science and Technology Project of Jiangsu Provincial Housing and Urban-Rural Construction Department (2018ZD088). This work is partly supported by the Natural Science Foundation of Jiangsu Province of China (No. BK20161165), the applied fundamental research Foundation of Xuzhou of China (No. KC17072). The authorized patents for invention are also the research and development of Jiangsu Province Industry-University-Research Cooperation Project (BY2019056).

References

1. Zhang, Z., Yao, K., Ma, C., Chen, J., Wu, C.: All-fixed switching frequency control of CRM boost PFC converter based on variable inductor in a wide input voltage range. In: 2019 IEEE Energy Conversion Congress and Exposition (ECCE). IEEE (2019)
2. Wu, Y., Ren, X., Zhou, Y., Chen, Q., Zhang, Z.: Dynamic AC line frequency response method for LUT-based variable on-time control in 360 Hz–800 Hz CRM boost PFC converter. IEEE Trans. Power Electron. **PP**(99), 1 (2020)

3. Chen, Y.L., Chen, Y.M., Chen, H.J.: On-time compensation method for CRM/DCM Boost PFC converter. In: 2013 Twenty-Eighth Annual IEEE Applied Power Electronics Conference and Exposition (APEC). IEEE (2013)
4. Yao, K., Zhang, Z., Yang, J., Liu, J., Shao, F.: Quasi-fixed switching frequency control of CRM boost PFC converter based on variable inductor in wide input voltage range. IEEE Trans. Power Electron. **PP**(99), 1 (2020)
5. Wei, X.F., Chen, S.Y., Zhu, H.K., Yang, X., Guo, X.: Research on high power density LLC resonant converter based on GaN device. Adv. Technol. Electr. Eng. Energy (2019)
6. Fang, Y., et al.: Research on novel bridgeless dcm pseudo-boost PFC converter. J. Electr. Eng.
7. Jang, P., Kang, S., Cho, B., et al.: Totem-pole bridgeless boost PFC converter based on GaN FETs. In: Power Electronics Annual Conference, pp. 185–186 (2014)
8. Yang, F.: Interleaved critical conduction mode boost PFC converter with coupled inductor. IEEE Trans. Power Electron. PE (2011)
9. Ren, X., Wu, Y., Guo, Z., Zhang, Z., Chen, Q.: An online monitoring method of circuit parameters for variable on-time control in CRM boost PFC converters. IEEE Trans. Power Electron. **32**, 1786–1797 (2019)
10. Gao, J.: Analysis of a boost PFC pre-regulator operated in both CRM and DCM (2015)
11. Yao, K., Liu, J., Zhu, D., Jin, Z.: High power factor CRM boost PFC converter with optimum switching frequency variation range control based on variable inductor. IEEE Trans. Power Electron. **PP**(99), 1 (2021)
12. Ren, X., Wu, Y., Chen, Q., Zhang, Z.: Accurate operation analysis based variable on-time control for 360 Hz–800 Hz CRM boost PFC converters. IEEE Trans. Ind. Electron. **PP**(99), 1 (2019)
13. Wu, Y., Ren, X., Li, K., Zhang, Z., Chen, Q.: An accurate variable on-time control for 400 Hz CRM boost PFC converters *. In: 2019 IEEE Applied Power Electronics Conference and Exposition (APEC). IEEE (2019)
14. Sun, J., Huang, X., Strain, N.N., Costinett, D.J., Tolbert, L.M.: Inductor design and ZVS control for a GaN-based high efficiency CRM totem-pole PFC converter. In: 2019 IEEE Applied Power Electronics Conference and Exposition (APEC). IEEE (2019)
15. Ren, X., Yu, W., Guo, Z., Zhang, Z., Chen, Q.: An online monitoring method of circuit parameters for variable on-time control in CRM boost PFC converters. IEEE Trans. Power Electron. **34**(99), 1786–1797 (2018)
16. Chen, Y.L., Chen, Y.M.: Line current distortion compensation for DCM/CRM boost PFC converters. IEEE Trans. Power Electron. **31**(3), 2026–2038 (2015)